

Time-reversal symmetry breaking in a square lattice

Kevin Jimenez and Jose Reslen

Coordinación de Física, Universidad del Atlántico, Carrera 30 Número 8-49, Puerto Colombia.

(Dated: September 24, 2020)

The bulk conductivity of a two-dimensional system is studied assuming that quantum interference effects break time-reversal symmetry in the presence of strong spin-orbit interaction and strong lattice potential. The study is carried out by direct diagonalization in order to explore the nonlinear-response regime. The system displays a quantized conductivity that depends on the intensity of the electric field and under specific conditions the conductivity limit at zero electric field shows a nonvanishing value.

I. INTRODUCTION

An essential result from quantum mechanics prescribes that when two operators commute there exists an eigenbasis that diagonalizes them simultaneously, so that the elements of such an eigenbasis conform at the same time to both operators. It is however important to highlight that this principle does not dictate that any eigenbasis of the first operator is also an eigenbasis of the other, which would automatically imply that any eigenstate of the first operator should conform to the second one. Nevertheless, such an implication takes place in one instance: When the spectrum of the first operator is non-degenerate. These facts are at the center of the theory of (standard) phase transitions: In a scenario where the Hamiltonian commutes with an unitary operator (generated by the symmetry) a critical point separates a trivial or symmetric phase, where the state conforms to both the Hamiltonian and the symmetry, from a non-trivial or broken phase, where the physical state is no longer a symmetry eigenstate. A transition of this kind is only possible when the Hamiltonian spectrum goes from non-degenerate to degenerate, being the latter case the only one where the physical state can break the symmetry. From this perspective a phase transition is essentially the arising (or suppression) of the Hamiltonian's degeneracy. The mechanisms by which the symmetry is broken must be on the one hand irreversible [1], since otherwise equilibrium states would retain the Hamiltonian's symmetries, and on the other hand global, so that they affect the state as a whole and the symmetry be broken everywhere. Without these mechanisms the symmetry would not break and the phase transition would not take place. A typical example of this kind of transition is

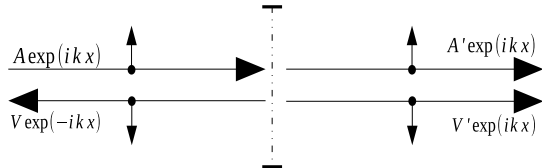


FIG. 1: Scattering model of a non-magnetic obstacle.

the change from paramagnetic (symmetric) to ferromagnetic (broken) in spin systems. In the case of electron systems, a paramount result known as the Kramers degeneracy [2] has significant implications in connection to phase transitions: Time-reversal spin-systems have degenerate spectra. As such, the notion of phase transition in this kind of systems cannot be accommodated in the standard symmetry-breaking paradigm associated with a transition from degenerate to non-degenerate or vice versa. However, it has been observed that a phase transition can take place whereupon the symmetry is broken *locally* in the non-trivial phase, i.e., some parts of the state, usually those associated with the system's bulk, display symmetry, but others, like those associated with the system's boundary, do not. This phase is known as the topological insulator[3–5]. In contrast, the trivial phase lacks symmetry-breaking mechanisms entirely, thus being known as the standard insulator. The symmetry associated with the transition is *time-reversal* (TR) [2], while the symmetry-breaking mechanism is *quantum interference*, which is generated by spin-orbit interaction. In order to appreciate the mentioned mechanism with some degree of formality, let us imagine a situation in which a spin-up electron moving forward bumps elastically into an obstacle, as portrayed in figure 1. The incident particle can be scattered in different ways but the case is such that the only state available for backscattering corresponds to spin down. The obstacle effect can be modeled by the following term

$$\hat{U}(x) = U(e^{i\frac{\theta}{2}\hat{\sigma}_1} + e^{-i\frac{\theta}{2}\hat{\sigma}_1})\delta(x), \quad \hat{\sigma}_1 = \begin{pmatrix} 0 & 1 \\ 1 & 0 \end{pmatrix}. \quad (1)$$

Notice that the effect is such that rotations in opposite directions by an angle θ are equally considered. This means the potential is TR invariant, i.e., it does not mutate under the change $t \rightarrow -t$ [17]. This case corresponds to a non-magnetic obstacle. The problem can be approached by considering solutions on each side of the obstacle following the decomposition shown in figure 1.

$$\psi_I(x) = A e^{ikx} |\uparrow\rangle + V e^{-ikx} |\downarrow\rangle, \quad (2)$$

$$\psi_{II}(x) = A' e^{ikx} |\uparrow\rangle + V' e^{ikx} |\downarrow\rangle. \quad (3)$$

Demanding wave function continuity, $\psi_I(0) = \psi_{II}(0)$, it is found that $A = A'$ and $V = V'$. Integration of the

Schrodinger equation around the origin yields

$$V \left(-\frac{ik}{m} + 2U \cos \frac{\theta}{2} \right) |\downarrow\rangle + 2UA \cos \frac{\theta}{2} |\uparrow\rangle = 0. \quad (4)$$

For finite values of U the only nontrivial solution is for $V = 0$ and $\theta = \pi$, which represents a spin-up state with perfect conduction in spite of the particle hitting an obstacle. Contrary to potential (1), this perfect conduction state is not TR invariant. This effect is produced by the destructive interference of backscattering paths and as such is a quantum-mechanical effect [4]. One of the causes of this result is the fact that backscattering is only possible via spin inversion. The existence of spin-flipped channels in opposite directions is guaranteed by the Kramers degeneracy as long as the Hamiltonian be TR invariant. Another determining factor is that only one forward-moving state as well as one backward-moving state are physically relevant. A similar effect could be obtained should the number of relevant moving channels in one direction be odd. Contrariwise, the suppression of backscattering paths due to quantum interference is unfeasible when the number of moving channels in one direction is even. This can be seen considering a Hamiltonian that displays the common form (the constant term $\vec{\sigma}^2$ is included only to keep a reference to spin states)

$$\hat{H} = \frac{\vec{p}^2}{2m} + U(\vec{x}) + \lambda \vec{\sigma}^2. \quad (5)$$

It then follows $\hat{H}|\vec{p}\rangle = \hat{H}|\vec{p}\rangle$. As a result, given an eigenstate with average momentum $\langle \vec{p} \rangle$ it is always possible to construct another eigenstate with the same energy, spin and spatial distribution, but opposite momentum $-\langle \vec{p} \rangle$, providing in this way direct backscattering channels. In this example the number of moving channels on each direction is always even, because every solution admits spin up and down. The correspondence between dissipation when there is an even number of moving channels and conduction when there is an odd number of moving channels can be represented using the members of the group $Z_2 = \{0, 1\}$. This equivalence has prompted the use of the adjective “topological” when referring to the case of nonvanishing conductivity. Also, it has been shown that it is possible to formally establish the classification of a given system from its Block energy-structure using topology methods [6].

One way of inhibiting even numbers of moving channels is to deliberately break the model’s TR invariance. The simplest strategy consists in applying a magnetic field to a spinless electron

$$\hat{H} = \frac{(\vec{p} - e\vec{A})^2}{2m} + U(\vec{x}). \quad (6)$$

In a two-dimensional space with perpendicular magnetic field the vector potential is given by $\vec{A} = (0, eB\hat{x})$. The

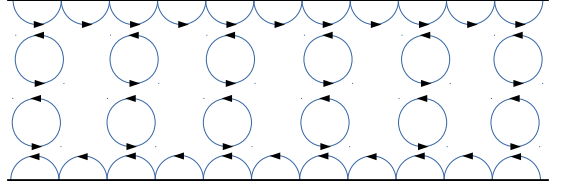


FIG. 2: Contrary to bulk states, boundary states on each edge break TR symmetry when considered separately.

associated term breaks the parity symmetry since it is not invariant under the change $\vec{x} \rightarrow -\vec{x}$. It can therefore be said that neither parity nor TR are independently preserved. However, assuming that $U(-\vec{x}) = U(\vec{x})$, it is noticeable that the Hamiltonian is invariant under parity and TR applied *simultaneously*. In absence of symmetry breaking mechanisms two possibilities arise. First, states that are invariant under parity must be invariant under TR too. These states compose the system’s bulk and are represented by circular orbits in figure 2. Second, states that break parity must break TR in such a way that the total state remain unchanged. These are the helical trajectories (edge states) on the system’s boundary shown also in figure 2. In this context, backward-moving states shift from forward-moving states, leaving only one moving channel on each edge and allowing the arising of an energy gap associated with backscattering as other elements of the problem, as for example an electric field or electron-electron collisions, are taken into account. As backscattering channels become sufficiently suppressed, motion on the edges becomes dissipationless. As can be seen, the conduction mechanism is rooted in the local breaking of the TR symmetry rather than in quantum interference, since in this example the Hamiltonian is not TR invariant. It is known that at low temperatures the transverse conductivity of (6) comes in integer multiples n of e^2/h [7, 8]. This phenomenon is known as the integer quantum Hall effect [9]. Number n has been shown to correspond to a topological invariant [10], which explains the notable robustness of the effect observed in experimental measurements. In a topological insulator dissipation channels are displaced just as in the Hall effect, but the role of the magnetic field is taken over by the spin, such that A. In the system’s boundary the number of moving channels in one direction is odd. And B. The Hamiltonian is TR invariant. These facts combined lead to the quantum interference that provokes the state to break TR symmetry and so become conducting [11, 12]. It is often said in this regard that conduction is “protected” by the TR symmetry. Topological insulators are peculiar in that they can conduct even though their bulk spectra are gaped.

The goal of the present study is to provide a numerical analysis of a single-body model where the symmetry-breaking takes place in the bulk, such that the role of the edge is replicated by a strong lattice potential. It is of interest to consider the electric field as an integral part

of the problem and to observe how the conductivity depends on this field beyond the linear approximation. This approach intends to shed insight by helping visualize the system's response as a complement to the more abstract analytical formulation often found in related studies. Interestingly, this procedure yields a quantized conductivity that shows a dependence with the number of bands below the Fermi energy and in some cases this conductivity remains finite as the electric field goes to zero, suggesting in this way a superconducting state.

II. THE MODEL AND ITS EIGENSYSTEM

The model corresponds to an electron that moves on a two-dimensional potential $U(x, y)$ under the action of an electric field E in the y direction. Spin-orbit interaction arises as a coupling between the z -components of spin and angular momentum. The Hamiltonian is written as

$$\hat{H} = \frac{\hat{p}_x^2 + \hat{p}_y^2}{2m} + \frac{\lambda}{m} \hat{\sigma}_z (\hat{x}\hat{p}_y - \hat{y}\hat{p}_x) + U(\hat{x}, \hat{y}) - eE\hat{y}. \quad (7)$$

Constants m and e represent mass and charge respectively. The intensity of the spin-orbit interaction is mediated by constant λ . The potential is written as

$$U(x, y) = U_x \cos \frac{2\pi x}{a} + U_y \cos \frac{2\pi y}{a} \quad (8)$$

Current technology allows for a high degree of control over the model's parameters in optical lattices or superlattices [13, 14], being these scenarios where the effects reported further ahead are more likely to be observed. For a numerical analysis it is necessary to bound the system in order to provide a compact Hilbert space, hence periodic boundary conditions are imposed on the x -axis over a square lattice of side L . Lattice constant a is such that $L = Na$, being N the square root of the total number of real unit-cells in the lattice. It can be noticed that due to the terms of spin-orbit and electric field, Hamiltonian (7) does not display translational invariance in neither axis and therefore it does not admit a treatment in terms of Bloch functions. However, it is possible to consider an alternative symmetry arising from simultaneous translations of space and momentum, but for this it is necessary to add a term, as follows

$$\hat{H}_0 = \hat{H} + \frac{\lambda^2 \hat{x}^2}{2m}. \quad (9)$$

The extra-term can be considered either as a physical confining potential, in which case it becomes an integral part of the Hamiltonian, or as a perturbation. Both (7) and (9) are TR invariant, but only (9) commutes with the following symmetry operator ($\hbar = 1$)

$$\hat{T} = e^{ia\hat{p}_x + ia\lambda\hat{\sigma}_z\hat{y}}. \quad (10)$$

This can be confirmed using $\hat{T}\hat{x}\hat{T}^{-1} = \hat{x} + a$ and

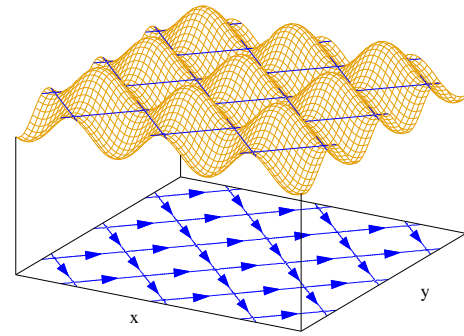


FIG. 3: Conduction channels take place around potential extrema giving rise to a net current in the x axis.

$\hat{T}\hat{p}_y\hat{T}^{-1} = \hat{p}_y - a\lambda\hat{\sigma}_z$. Fundamental results dictate that there exists a common basis for \hat{H}_0 and \hat{T} . The most general way of writing an eigenfunction of \hat{T} with eigenvalue e^{ika} is

$$\psi(x, p_y, \sigma_z) = e^{ikx} u_k(x, p_y, \sigma_z), \quad (11)$$

subject to the condition $u_k(x + a, p_y - a\lambda\sigma_z, \sigma_z) = u_k(x, p_y, \sigma_z)$. These requirements are met for functions defined as

$$u_k(x, p_y, \sigma_z) = \sum_{j,w} C_{j,w,\sigma_z}(k) e^{j\frac{2\pi i}{L}x} e^{-w2\pi i p_y} \begin{bmatrix} \delta_1^{\sigma_z} \\ \delta_{-1}^{\sigma_z} \end{bmatrix}, \quad (12)$$

insofar as

$$\frac{j}{L} + w\lambda\sigma_z = \frac{n}{a}, \quad (13)$$

being n an arbitrary integer. Solving for w yields

$$w = \frac{q}{\lambda L \sigma_z}, \quad (14)$$

being $q = nN - j$. Integer j is not bounded, since the corresponding momentum eigenvalue $p_x = \frac{2\pi j}{L}$ in (12) remains always consistent with boundary conditions. This is not the case for the position eigenvalue $y = 2\pi w$ because the system is bounded on the y axis, therefore

$$|2\pi w| \leq \frac{L}{2}. \quad (15)$$

Using (14) it then follows

$$q_{max} = \frac{\lambda L^2}{4\pi}. \quad (16)$$

Since q in (14) can take negative values, the total number of position states is given by $Q = 2q_{max} + 1$. Inserting Q and solving for L gives

$$L = \sqrt{\frac{2\pi(Q-1)}{\lambda}}. \quad (17)$$

As a consequence, the system length depends on the number of states and the interaction constant. This conditioning certainty arises from the symmetry and seems to be related to the fact that Heisenberg's uncertainty principle establishes a phase space grating. Another result is that the system's eigenfunctions are periodic in the p_y -space with period λL , as can be seen from (14) and (12). Besides, periodic boundary conditions on the x axis $\psi(x+L, p_y) = \psi(x, p_y)$ determine as valid values of $k = \frac{2\pi l}{L}$, for l integer. The size of a unit cell in k -space is $\frac{2\pi}{a}$. The eigenvalue problem can be formulated in terms of the symmetry functions as

$$|\hat{H}_k u_k\rangle = \mathcal{E}|u_k\rangle, \quad (18)$$

wherein

$$\begin{aligned} \hat{H}_k = e^{-ik\hat{x}} \hat{H}_0 e^{ik\hat{x}} &= \frac{(\hat{p}_x + k)^2}{2m} + \frac{(\hat{p}_y + \hat{\sigma}_z \lambda \hat{x})^2}{2m} + \\ &- \frac{\lambda}{m} \hat{\sigma}_z \hat{y} (\hat{p}_x + k) + U(\hat{x}, \hat{y}) - eE\hat{y}, \end{aligned} \quad (19)$$

being \mathcal{E} the system's energy. As the problem is separable with respect to spin, it is valid to set $\hat{\sigma}_z = 1$ in order to focus on the spin-up case. Technically, the resulting expression breaks TR symmetry, but the operation is justified by the fact that quantum interference breaks such a symmetry through the same quantum interference effect that takes place in the boundary of a topological insulator, with the difference that in this case the role of the boundary is taken over by the periodic potential, which must in addition be sufficiently strong to induce trajectories surrounding potential peaks in the bulk, as sketched in figure 3. Since \hat{x} and \hat{p}_y are to be used as a complete set of commuting observables, the following results must be considered, $p_x = -i\partial_x$, $y = i\partial_{p_y}$. Basis functions are taken as eigenfunctions of \hat{p}_x and \hat{y} normalized over the xp_y -cell

$$\langle x, p_y | j, q \rangle = \phi_{j,q}(x, p_y) = \frac{e^{j\frac{2\pi}{L}x} e^{-q\frac{2\pi}{\lambda L}p_y}}{L\sqrt{\lambda}}. \quad (20)$$

Calculation of the matrix elements, $\langle j', q' | \hat{H}_k^\dagger | j, q \rangle$, yields

$$\begin{aligned} &\int_{-\frac{L}{2}}^{\frac{L}{2}} dx \int_{-\frac{\lambda L}{2}}^{\frac{\lambda L}{2}} dp_y \phi_{j', q'}^*(x, p_y) H_k^\dagger \phi_{j, q}(x, p_y) = \\ &\frac{1}{2m} \left(\frac{2\pi j}{L} + k \right)^2 \delta_{j'}^j \delta_{q'}^q + \frac{\lambda^2 L^2}{4\pi^2 m} \left(f(q, q') \delta_{j'}^j + \right. \\ &g(q, q') g(j, j') + f(j, j') \delta_{q'}^q \Big) - \frac{2\pi q}{mL} \left(\frac{2\pi j}{L} + k \right) \delta_{q'}^q \delta_{j'}^j \\ &+ \frac{U_x}{2} (\delta_N^{j-j'} + \delta_{-N}^{j-j'}) \delta_{q'}^q + U_y \cos \frac{4\pi^2 q}{a\lambda L} \delta_{j'}^j \delta_{q'}^q + \\ &- eE \frac{2\pi q}{\lambda L} \delta_{q'}^q \delta_{j'}^j, \end{aligned} \quad (21)$$

where

$$f(n, n') = \begin{cases} \frac{\pi^2}{6} & \text{if } n = n', \\ \frac{(-1)^{n-n'}}{(n-n')^2} & \text{if } n \neq n', \end{cases} \quad (22)$$

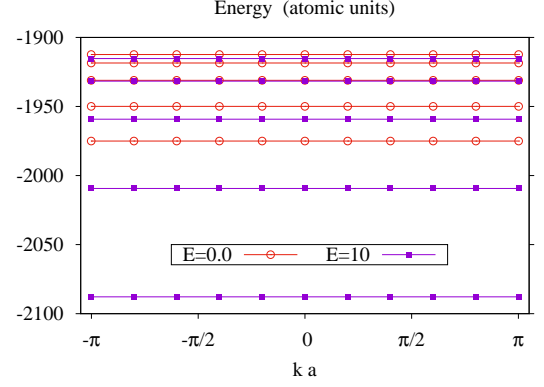


FIG. 4: First bands of Hamiltonian (21) for extreme values of the electric field. The model constants in atomic units are $m = 1$, $e = 1$, $\lambda = 1$, $U_x = U_y = 10^3$ and $L = 25.1$. Additionally $N = 10$, $Q = 101$ and $J = 201$. The band pattern is notably flat along a wide range of values of E . Because the lattice potential is strong this system would be a standard insulator in absence of spin-orbit interaction.

and

$$g(n, n') = \begin{cases} 0 & \text{if } n = n', \\ \frac{(-1)^{n-n'}}{n-n'} & \text{if } n \neq n'. \end{cases} \quad (23)$$

Interestingly, matricial elements are all real even though the basis functions are complex. This helps reduce computation costs. When this Hamiltonian is numerically diagonalized the respective eigenfunctions take the next form

$$|u_k\rangle = \sum_{q=-q_{max}}^{q_{max}} \sum_{n=-n_{max}}^{n_{max}} c_{j,q}(k) |j, q\rangle. \quad (24)$$

The momentum integer is $j = Nn - q$ and the total number of momentum states is $J = 2n_{max} + 1$. Figure 4 presents the first bands of the Hamiltonian for a set of reasonable parameters and strong lattice potential. In addition to being flat, the band pattern is nondegenerate, which indicates the number of states in one direction must be odd (one). Given the TR symmetry of the whole Hamiltonian, it is viable to assume that the quantum interference mechanisms that take place in the boundary of a topological insulator also take place in this system.

III. CONDUCTIVITY

The mean values of momentum and position over state (11) are

$$\langle \hat{p}_x \rangle_k = k + \sum_{j,q} |c_{j,q}(k)|^2 \frac{2\pi j}{L} \quad (25)$$

Taking the effect of electron-electron collisions as a perturbation, it can be said that at zero temperature the

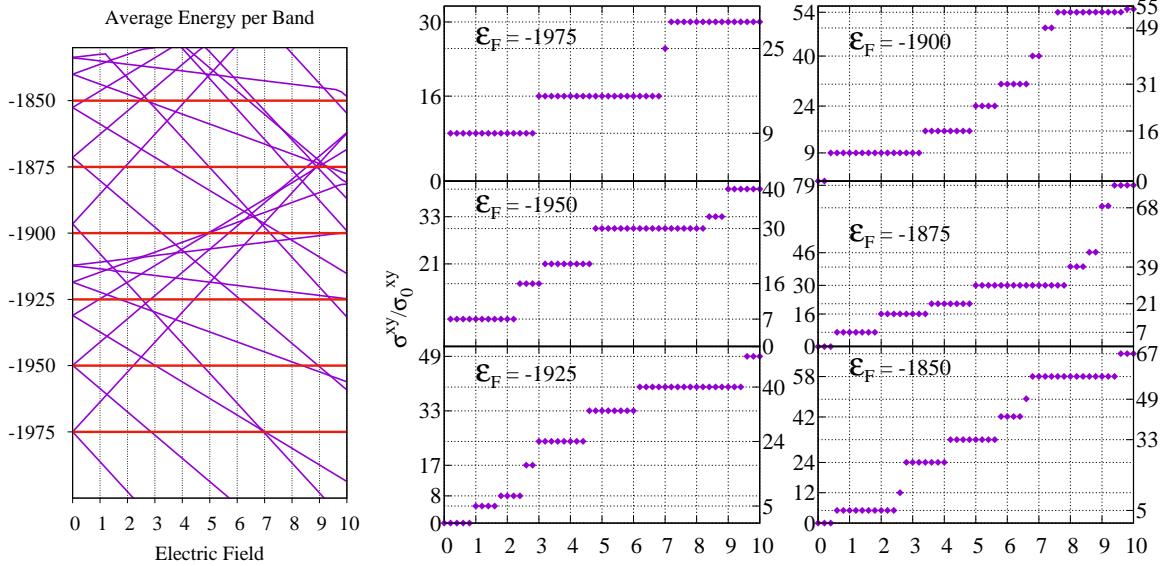


FIG. 5: Left. Average value of energy over each band vs electric field, both in atomic units. Red lines show the Fermi levels considered on the right. Right. Zero-temperature transverse-conductivity $\sigma^{xy}/\sigma_0^{xy}$ vs Electric Field (atomic units) for different values of the Fermi level. It can be seen that conductivity always comes in integer multiples of σ_0^{xy} . Comparing with the graph on the left it can be seen that the conductivity jumps every time a band crosses the respective Fermi level. The system's parameters are indicated in the caption of figure 4. For these parameters the reference value $\sigma_0^{xy} = 13.78\alpha$ was found analysing the conductivity data. The cases $\epsilon_F = -1975$ and $\epsilon_F = -1950$ are distinctive in that in the limit of zero electric field conductivity is nonvanishing.

contribution of a given band to the x -conductivity is at first order proportional to the sum of momentum mean values over that band

$$\Pi_x^{band} = \sum_{l=-\frac{N}{2}}^{\frac{N}{2}} \langle \hat{p}_x \rangle_{k=\frac{2\pi l}{L}}. \quad (26)$$

The transverse conductivity is proportional to the sum of contributions from all the bands below the Fermi level ϵ_f

$$\sigma^{xy} = \alpha \sum_{band < \epsilon_f} \Pi_x^{band}. \quad (27)$$

Being α a proportionality constant. Figure 5 shows energy as well as conductivity against electric field. It can be seen that σ^{xy} comes in integer multiples of a constant that shows no dependence with the electric field. This conductivity displays a stair pattern, being constant over intervals of different extension and increasing by integer steps of different size in the same points where a given band crosses the corresponding Fermi energy as the electric field grows. The stair pattern became less appreciable in simulations with smaller λ . In the quantum Hall effect, the integer that determines the conductivity is given by the number of times the wave-function phase winds around the boundary of a two-dimensional Brillouin zone [7, 10]. Such an integer is known in topology as the Chern invariant [3]. This parallel does not apply

here since the inclusion of the electric field in the Hamiltonian breaks translational invariance in the y -axis and the reciprocal lattice becomes one-dimensional. Whether there are additional topology constructs that apply in this context or the system's discreteness can be ascribed to deeper precursors remains to be seen. Whatever the case, this result shows that the conductivity's quantization does not depend on the linear-response assumptions necessary to obtain the Kubo formula [7, 15]. Another curious trait of figure 5 is that for the lowest two values of Fermi energy conductivity features finite limits at zero electric field. For this to happen the Fermi energy must equal one of the system's energy values for vanishing electric field. This limit is consistent with a superconductor state because it features dissipationless conduction on account of the quantum interference effect already discussed in this document. It would then be interesting to add a magnetic field to Hamiltonian (9) and see whether this magnetic field is offset by the induced magnetization, giving in this way a solid evidence of the superconducting state.

Contrary to transversal conductivity, the first order longitudinal conductivity vanishes for any electric field. This happens because the system displays backscattering channels in the y -axis,

$$\hat{H}_0|x, p_y, s_z\rangle = \hat{H}_0|-x, -p_y, s_z\rangle. \quad (28)$$

These channels are nonetheless displaced, so that TR symmetry is broken locally just as in the Hall effect. By

a similar mechanism, longitudinal conductivity could be induced adding an electric field in the x -axis. Likewise, the inclusion of interaction terms directly in the Hamiltonian would open a gap between the states involved in (28), since dissipation channels are spatially separated and a particle would normally experience collisions in going from x to $-x$ in proportion to the magnitude of x . The same phenomenon can also explain the longitudinal conduction in topological insulators [16]. Although interaction terms were not considered in this work, the single body functions obtained in section II are the starting point to build a second-quantization Hamiltonian giving a more accurate representation of the system, in which case it is reasonable to expect nonvanishing longitudinal conduction.

IV. CONCLUSIONS

A single-body spin-orbit interaction model has been used to study the conductivity pattern produced by a symmetry-breaking mechanism that takes place in the system's bulk. The electric field responsible for charge transport has been included in the Hamiltonian and the study has been carried out by direct diagonalization in order to explore the system's response beyond the linear approximation. Such a response displays a discrete

pattern that is consistent with the quantization of conductivity over the range of fields considered in the study, showing in this way that a quantized conductivity can be observed in the non-linear regime. The quantization value is found to depend on the number of energy bands located below the system's Fermi energy and also on the intensity of the electric field. In the particular case of the Fermi energy being equal to an eigenenergy of the zero-field Hamiltonian, the limit of conductivity for vanishing electric fields proves to be finite. This feature is consistent with a superconducting state but additional tests are necessary to confirm such a hypothesis. Were it verified, it would mean the mechanism by which the TR symmetry in broken in a superconductor is the same than the one taking place in the edges of topological insulators. Overall, both the system's physics as well as the perspective granted by the numerical analysis display interesting features.

V. ACKNOWLEDGMENTS

Financial support from Vicerrectoría de Investigaciones, Extensión y Proyección Social from Universidad del Atlántico through the program Investigación Formativa is gratefully thanked by both authors.

[1] K. Jimenez and J. Reslen *Thermodynamic signatures of an underlying quantum phase transition: A grand canonical approach* Physics Letters A **380** 2603 (2016).

[2] J. Sakurai *Modern quantum mechanics revised edition*

[3] M. Hasan and C. Kane *Colloquium: Topological insulators* Reviews of Modern Physics **82** 3045 (2010).

[4] X. Qi and S. Zhang *The quantum spin Hall effect and topological insulators* Physics Today **63** 1 33 (2010).

[5] X. Qi and S. Zhang *Topological insulators and superconductors* Reviews of Modern Physics **83** 1057 (2011). Addison-Wesley Publishing Company (1994).

[6] C. Kane and E. Mele *Z_2 Topological Order and the Quantum Spin Hall Effect* Physical Review Letters **95** 146802 (2005).

[7] D. Thouless, M. Kohmoto, M. Nightingale and M. den Nijs *Quantized Hall conductance in a two-dimensional periodic potential* Physical Review Letters **49** 405 (1982).

[8] R. Laughlin *Quantized Hall conductivity in two dimensions* Physical Review B **23** 5632 (1981).

[9] J. Sinova, S. Valenzuela, J. Wunderlich, C. Back and T. Jungwirth *Spin Hall effects* Review of Modern Physics **87** 1213 (2015).

[10] M. Kohmoto *Topological invariant and quantization of the Hall conductance* Annals of Physics **160** 343 (1985).

[11] P. Roushan, J. Seo, C. Parker, Y. Hor, D. Hsieh, Dong Qian, A. Richardella, M. Hasan, R. Cava and A. Yazdani *Topological surface states protected from backscattering by chiral spin texture* Nature **460** 1106 (2009).

[12] T. Zhang, P. Cheng, X. Chen, J. Jia, X. Ma, K. He, L. Wang, H. Zhang, X. Dai, Z. Fang, X. Xie and Q. Xue *Experimental demonstration of topological surface states protected by time-reversal symmetry* Physical Review Letters **103** 266803 (2009).

[13] V. Galitski and I. Spielman *Spin-orbit coupling in quantum gases* Nature **494** 49 (2013).

[14] S. Kolkowitz, S. Bromley, T. Bothwell, M. Wall, G. Marti, A. Koller, X. Zhang, A. Rey and J. Ye *Spin-orbit-coupled fermions in an optical lattice clock* Nature **000** 1 (2016).

[15] R. Kubo *Statistical-mechanical theory of irreversible processes. I. General theory and simple applications to magnetic and conduction problems* Journal of the physical society of Japan **12** 570 (1957).

[16] M. Konig, S. Wiedmann, C. Brune, A. Roth, H. Buhmann, L. W. Molenkamp, X. L. Qi and S. C. Zhang *Quantum Spin Hall Insulator State in HgTe Quantum Wells* Science **318** 766 (2007).

[17] This provokes $\hat{\sigma}_1 \rightarrow -\hat{\sigma}_1$